*Design of Machines and Structures, Vol. 2, No. 2 (2012), pp. 123–135.*
*https://doi.org/10.32972/dms.2012.020*

# ANALYTICAL MODEL TO DETERMINE MESHING STIFFNESS OF SPUR GEARS

RENÁTA SZŰCS–LÁSZLÓ KAMONDI
Department of Machine and Product Design, University of Miskolc
H-3515 Miskolc-Egyetemváros
szucs.renata@citromail.hu; machkl@uni-miskolc.hu

**Abstract.** During dynamic analysis of gears correct determination of the meshing stiffness bears great importance. In order to determine meshing stiffness first of all the contact points have to be located. In this work a general method is presented for determining the contact points i.e. the contact curve, and a special method for involute profiles. An analytical method for deflection analysis of spur gears is formulated. During deflection analysis elastic deformation of the teeth is taken into account and as a consequence of the model and the calculation method failure in the base pitch and the profile can be treated.

**Keywords:** gear mesh, meshing stiffness, elastic deflection, non-linear dynamics

## 1. INTRODUCTION

Due to the increasing demands analysis of reasons of noise sources and dynamic effects is important, it is also indicated by the numbers of works published even nowadays in this area. On one hand installation inaccuracies and on the other hand elastic deformation of the teeth and base pitch and profile errors are the most common reasons of the undesired dynamic effects.

Endeavour to increase volume performance and service life of drive gears results in installation of gears of smaller accuracy grade. In case of these accuracy grades scale of elastic deformations and teeth errors can be the same. In order to decrease the disturbing effect of elastic deformation trimming of the tooth tip is a common procedure, but from the point of analysis of stress conditions, knowing deflections of the tooth at the whole contact region is essential.

Before wide-spreading of computers only analytical methods were available for deflection analysis. In that time authors [Karas, Weber] modelled the tooth as a cantilever. Between these models the main difference was the description of the tooth profile i.e. some models only approximate the involute curve, while others deal with the real curve. Of course these models vary on approximation of other conditions too. Nowadays papers dealing with tooth deflection of external spur gears can be divided into two main groups. Studies belonged to the first groups [2–5] model the tooth as a cantilever beam even nowadays, but owing to development of calculation and modelling methods approximations are more accurate and on the other hand in most cases authors supplement their results with FEA analysis. Studies of the second group [6–9] use FEM analysis for determine tooth deflection of gears. Regarding the considered and neglected stresses (e.g. pressing, bending, shearing) causing deflection studies also differ from each other.

By the help of Finite Element Method analysis of gears is realizable in 3Ds, but it bears more importance in case of helical gears. From this point of view authors study tooth deflection by analytical methods in which the tooth is modelled by a cantilever, in this work

this method is presented in case of involute profiles. In this paper the model established by the authors neglects installation inaccuracies and friction, only takes into account the effects of elastic deformation. In later studies our aim is to verify results of this paper by FEM.

## 2. DYNAMIC MODELL

For dynamic analysis of gear drives a model shown in *Figure 1* has been developed [10, 11, 12]. The driver and the driven gear are modelled by masses rotating around the central points of the gears, while meshing is modelled by an equivalent spring and a damping proportional with the velocity in the direction of line of action. This model contains backlash which is neglected from the point of contact analysis at this stage. The model neglects friction and installation inaccuracies.

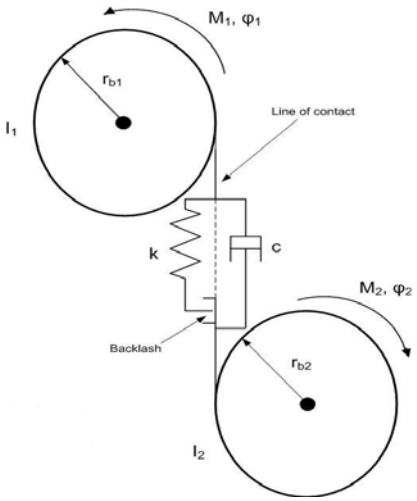



*Figure 1. Dynamic model*

Apart from development for the equation of motion the following relation can be written:

$$m \cdot \ddot{x} + c \cdot \dot{x} + k(t) \cdot h(x) = f_T(t) + f_M(t), \tag{1}$$

where:

$$m = \frac{I_1 \cdot I_2}{I_1 \cdot r_{b2}^2 + I_2 \cdot r_{b1}^1}, \tag{2}$$

$$f_T(t) = \frac{r_{b1} \cdot I_2 \cdot M_1 - r_{b2} \cdot I_1 \cdot M_2}{I_1 \cdot r_{b2}^2 + I_2 \cdot r_{b1}^2}, \tag{3}$$

$$f_M(t) = -m \cdot \ddot{e}(t), \tag{4}$$

$$h(x) = \begin{cases} x - b, & x \geq b \\ 0, & |x| > b \\ x + b, & x \leq -b \end{cases}. \tag{5}$$

*Table 1*

*List of symbols and parameters*

| | |
|---|---|
| $I_1, I_2$ | moments of inertia |
| $\varphi_1, \varphi_2$ | rotational angles |
| $x = r_{b1}\varphi_1 - r_{b2}\varphi_2$ | relative displacement |
| $r_{b1}, r_{b2}$ | radii of base circles |
| $M_1, M_2$ | external torques |
| 2b | whole backlash |
| c | damping |
| k(t) | meshing stiffness |
| e(t) | static transmission error |

Aim of this study is to determine meshing stiffness [k(t)], in order to introduce it into equation (1) for further works.

## 3. MESHING CONDITIONS

Determining of contact points is essential in order to calculate meshing stiffness during the course of meshing. In this section a general method and a special procedure adaptable to involute profiles can be found for contact analysis.

### 3.1. General tooth profile

Supposing that that curves of the mating gear profiles are known for determining the law of motion well-elaborated methods are available [1]. During the solution of this problem three coordinate systems should be employed, two of them are moving coordinate systems ($S_1$, $S_2$) rigidly connected to gear 1and gear 2 respectively (centre of gear 1 and 2 are $O_1$ and $O_2$). The third coordinate system is a fixed coordinate system, which is in rigid connection with the frame. Then equations of the individual tooth profiles and their normal vectors are prescribed in their own moving coordinate systems:

$$\boldsymbol{\rho_i} = \boldsymbol{\rho_i}(u_i) \qquad i = 1{,}2\,, \tag{6}$$

$$\boldsymbol{e_i} = \boldsymbol{e_i}(u_i) \qquad i = 1{,}2 \tag{7}$$

Let us transform eq. (5) and eq. (6) into the fix coordinate system S. In the function of individual rotational angles $\varphi_1$, $\varphi_2$ equations of the tooth profiles and the normal vectors are given:

$$\boldsymbol{\rho}^{(i)} = \boldsymbol{\rho}^{(i)}(u_i, \varphi_i) \qquad i = 1{,}2\,, \tag{8}$$

$$\boldsymbol{e}^{(i)} = \boldsymbol{e}^{(i)}(u_i, \varphi_i) \qquad i = 1{,}2 \tag{9}$$

If the two gears are in contact, both the radius vectors of these two profiles and both the basic vectors of the normal profiles should be the same, supposing the same orientation:

$$\boldsymbol{\rho}^{(1)}(u_1, \varphi_1) = \boldsymbol{\rho}^{(2)}(u_2, \varphi_2) \tag{10}$$

$$\boldsymbol{e}^{(1)}(u_1, \varphi_1) = \boldsymbol{e}^{(2)}(u_2, \varphi_2) \tag{11}$$

Solving equation (7) and (8) three independent scalar equations can be obtained. Knowing rotational angle $\varphi_1$, as the function of this angle, displacement function can be determined.

As a consequence of the fore-mentioned in case of general, prescribed profile curves determination of contact points is possible and so based on deflection analysis (See in Section 4) calculation of meshing stiffness.

### 3.2. Involute profile

Still nowadays one of the most widely used gear profile is involute. So analysis of the involute profile as a special case is reasonable. Compared to the general case for involute tooth profile several simplifications can be applied. The biggest advantage is that the contact curve is a line with direction angle of working pressure angle $\alpha_w$ and, which passes though point C (pitch point). Theoretically meshing can take place on this line between point A and E. The tooth contact begins at point A and terminates at point E during the course of tooth contact. Points A and E are intersected by the addendum circles of the respecting gears. In a given moment of the mesh by producing the mating involute profiles their pedal points can be obtained in the base circle (e.g. E – $B_{E2}$) (See *Figure 2*). Selecting the mating at point C as a base, any of the mating positions can be described by these pedal angles ($\alpha_{E2}$).

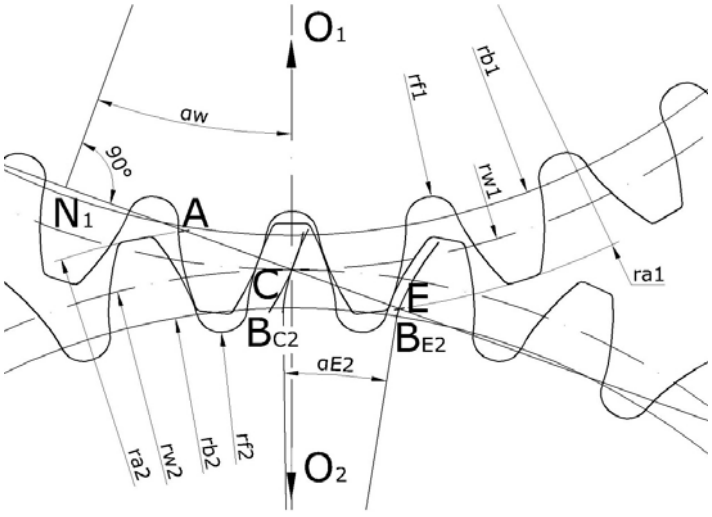



*Figure 2. Contact line in case of error-free, involute profile*

Since we assumed that the geometrical dimensions of the gears are known the tooth thickness measured at the working circle ($s_w$) is also known. Coordinates of the profile are established from profile point P, located at the working circle.

An arbitrary point of the tooth profile is J, and j presents its motion during the contact. Position of J$^j$ related to point P can be described by $\alpha_J^j$ (See *Figure 3*). Variation of $\alpha_J^j$ also describes meshing.

Coordinates $x_J^j, y_J^j$ of an arbitrary point J$^j$ can be determined by angles $\psi_J^j$, $\alpha_J^j$ and by the radius of the base circle ($r_b$):

$$x_J^j = \frac{r_b}{cos\alpha_J^j} sin\psi_J^j \,, \tag{12}$$

$$y_J^j = \frac{r_b}{cos\alpha_J^j} cos\psi_J^j \,. \tag{13}$$

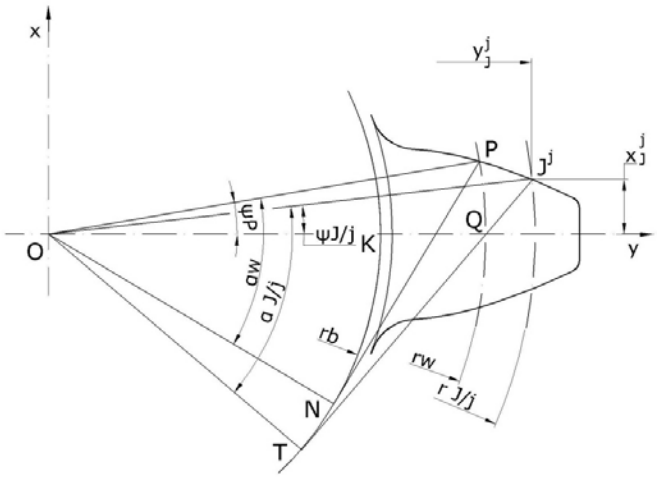



*Figure 3. Explanation of point* J$^j$

Angle $\alpha_J^j$ belonged to point $J^j$ can be determined by distance $\overline{J^jT}$ and by the radius of the base circle ($r_b$):

$$\alpha_J^j = \frac{\overline{J^jT}}{r_b} = \frac{\overline{PN} + \overset{\frown}{NT}}{r_b}. \tag{14}$$

Angle $\Psi_J^j$ determining location of point $J^j$ can be calculated by the help of tooth thickness of the working circle. While angle $\psi_p$ ($POx\sphericalangle$) can be determined as

$$\Psi_p = \frac{s_w}{2r_w}, \tag{15}$$

where: $\overline{PQ} = 0{,}5 \cdot s_w$.

According to the fore-mentioned we can establish the following relation for angle $\Psi_J^j$:

$$\Psi_J^j = \Psi_P + inv\Psi_P - inv\alpha_J^j. \tag{16}$$

By continuous change of angle $\alpha_J^j$ coordinates of the involute profile can be determined from the addendum circle to the limit circle. It is important because in fact meshing not only in the AE region can intervene but before point A and after point E. By the help of this method the whole gear profile can be described while mesh at the root curve does not intervene.

## 4. DETERMINATION OF DEFLECTIONS

The tooth is considered to be elastic and modelled as a non-uniform cantilever embedded through its width b. Cross section of the cantilever is changing in the function of the tooth width at the relevant point. The mating tooth pair is loaded by nominal load $F_N$. Due to this load the tooth deflects and flattens at the point of contact. This deformation results that the angular rotation determined by the gear ratio differ from the real gear ratio since the axis of the driven gear differ from the axis of the driver gear.

### 4.1. Model of the tooth and introduction of parameters

Deformation arising from different deflections is determined as the resultant of the "individual" tooth sections, because deflection depends on location of fulcrum of the load, i.e. instantaneous contact point. Deformation arising from interpenetration is determined aggregately to the whole tooth as it roughly constant along the contact path.

Deformation of the mating teeth is determined by the resultant of displacements in direction of the line of action.

As a result of the normal force the following displacements projected to direction of the line of action can be determined:

- $\delta_{Ja}^j$: from bending,
- $\delta_{Jb}^j$: from shearing,
- $\delta_{Jp}^j$: from pressing,
- $\delta_{Jc}^j$: fillet-foundation,
- $\delta_{Jd1,2}^j$: contact deflection.

In this study we neglect defection due to pressing, in the following we only take into account the remaining four elements.

For calculation of these deformation we divided cross section of the tooth into n segments which height is $y_k - y_{k-1}$, and length is $x_k$ as shown in *Figure 4*. For the segment $s_k$ we get

$$\overline{I_k} = \frac{I_k + I_{k-1}}{2}, \tag{17}$$

$$I_k = \frac{1}{12} b(2x_k)^3, \tag{18}$$

$$\overline{I_k} = \frac{b}{3}(x_k^3 - x_{k-1}^3) \tag{19}$$

where b is the width of the tooth and I is the moment of inertia.

Areas of the segments are given by:

$$\overline{A_k} = \frac{A_k + A_{k-1}}{2} \tag{20}$$

$$A_k = 2bx_k, \tag{21}$$

$$\overline{A_k} = b(x_k + x_{k-1}), \tag{22}$$

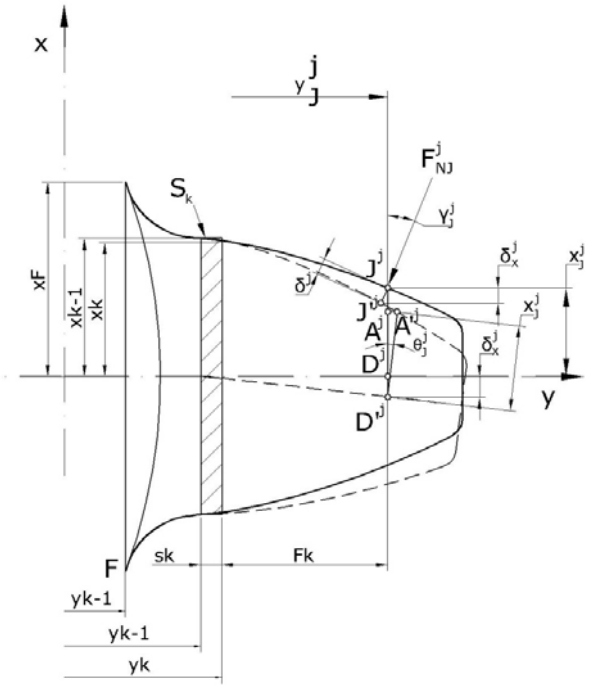



*Figure 4. Model of the tooth*

Division is made from the addendum circle to the place of fixation (point F), number of segments (n) should be determined in the function the mating conditions.

Load acts at point $J^j$ according to the contact. As *Figure 4* shows, distance between the fulcrum of the load and section k is designated by $F^k$, which is expressed by:

$$F_k = y_J^j - y_k. \tag{23}$$

Height of cross section of the tooth can be obtained as:

$$s_k = y_k - y_{k-1}. \tag{24}$$

Supposing plain stress condition, i.e. along face stress is zero, principal strain directions and principal stress direction are coincided, we can introduce elasticity module depending on Poisson ratio (υ):

$$E_\upsilon = \frac{E}{1-\upsilon^2}. \tag{25}$$

### 4.2. Bending deflection

Component $F_{NJ}^j \cdot cos\gamma_J^j$ of load $F_{NJ}^j$ acting at point $J^j$ bends and shears the tooth, while concentrated moment $F_{NJ}^j \cdot sin\gamma_J^j \cdot x_J^j$ at point $D_J^j$ bends the tooth in opposite direction. We note that load component $F_{NJ}^j \cdot sin\gamma_J^j$ subjects the tooth to compression load, but it is ignored as it was mentioned in Section 1.

Deformation can be calculated from balance of the external and internal forces.

Let us treat the tooth rigid from fulcrum of the load to section *k* and segment while segment $s_k$ is considered to be elastic. According to [14] strain in direction *x* of point $D_j$ and rotation of the neutral plane can be calculated.

For stain $\delta_{xa1}^{j,k}$ arising from the bending caused by component $F_{NJ}^j \cdot cos\gamma_J^j$ we get:

$$\delta_{xa1}^{j,k} = \frac{F_{NJ}^j \cdot cos\gamma_J^j \cdot s_k}{6E_\upsilon \bar{I}_K}(2s_k^2 + 5F_K s_K + 3F_K^2), \tag{26}$$

for rotation of the neutral plain:

$$\theta_{J1}^{j,k} = \frac{F_{NJ}^j \cdot cos\gamma_J^j \cdot s_k}{2E_\upsilon \bar{I}_K}(s_k + 2F_K). \tag{27}$$

For stain of $D_j$ ($\delta_{xa2}^{j,k}$) arising from the concentrated moment we have:

$$\delta_{xa,2}^{j,k} = -\frac{F_{NJ}^j \cdot sin\gamma_J^j \cdot x_J^j \cdot s_k}{2E_\upsilon \bar{I}_K}(s_K + 2F_K), \tag{28}$$

while angular rotation $\theta_{J2}^{j,k}$ is

$$\theta_{a2}^{j,k} = -\frac{F_{NJ}^j \cdot sin\gamma_J^j \cdot x_J^j \cdot s_k}{E_\upsilon \bar{I}_K}. \tag{29}$$

Accomplishing calculations, resultant strain and angular rotation can be expressed according to the following equations:

$$\delta_{xa1}^{j} = \frac{F_{NJ}^j \cdot cos\gamma_J^j}{6E_\upsilon}\sum_{k=1}^{N}\frac{s_k}{\bar{I}_k}(2s_k^2 + 5F_K s_K + 3F_K^2), \tag{30}$$

$$\theta_{J1}^{j} = \frac{F_{NJ}^{j} \cdot cos\gamma_J^j}{2E_v} \sum_{k=1}^{N} \frac{s_k}{\overline{I_K}} (s_k + 2F_K), \tag{31}$$

$$\delta_{xa,2}^{j} = -\frac{F_{NJ}^{j} \cdot sin\gamma_J^j \cdot x_J^j}{2E_v} \sum_{k=1}^{N} \frac{s_k}{\overline{I_k}} (s_K + 2F_K), \tag{32}$$

$$\theta_{a2}^{j} = -\frac{F_{NJ}^{j} \cdot sin\gamma_J^j \cdot x_J^j}{E_v} \sum_{k=1}^{N} \frac{s_K}{\overline{I_k}}. \tag{33}$$

Strain in direction of the line of contact is given by

$$\delta^j = \delta_x^j \cdot cos\gamma_J^j, \tag{34}$$

where $\delta_x^j = \overline{J^j A^j} - \overline{C^j A^j}$.

Resulting from triangle $A_jA'_jD'_j$: $\overline{C^j A^j} = x_J^j \cdot \theta_J^j \cdot tg\gamma_J^j$.
Recalling eq. (34) we can write:

$$\delta^j = \delta_{xi}^j \cdot cos\gamma_J^j - x_J^j \cdot \theta_J^j \cdot sin\gamma_J^j, \tag{35}$$

where i=a, b, c.

Substituting equations (30-33) into eq. (35) strain is then:

$$\delta_{Ja}^{j} = \frac{F_{NJ}^{j}}{E_v}\left[\frac{cos^2\gamma_J^j}{6} \sum_{k=1}^{N} \frac{s_k}{\overline{I_K}} (2s_k^2 + 5F_k s_k + 3F_k^2) - cos\,\gamma_J^j sin\gamma_J^j \cdot x_J^j \sum_{k=1}^{N} \frac{s_k}{\overline{I_k}} (s_k + 2F_k) + sin^2\gamma_J^j \cdot (x_J^j)^2 \sum_{k=1}^{N} \frac{s_k}{\overline{I_k}}\right], \tag{36}$$

where

$$\delta_{xa}^{j} = \delta_{xa1}^{j} + \delta_{xa2}^{j} \; and \; \theta_J^j = \theta_{J1}^{j} + \theta_{J2}^{j}. \tag{37}$$

### 4.3. Shearing deflection

Component $F_{NJ}^{j} \cdot cos\gamma_J^j$ of the load $F_{NJ}^{j}$ acts as a shearing force which procudes deformation of the tooth in direction x. As a consequence of nature of the deformation segment of the tooth between $Y_k$ and $Y_{k-1}$ behaves as a rigid element so it displaces in the direction of axis x, but it is not subjected to angular rotation.

According to [14] displacement for the $k^{th}$ segments can written as

$$\delta_{xb}^{j,k} = \frac{1{,}2F_{NJ}^{j} \cdot cos\gamma_J^j \cdot s_k}{G \cdot \overline{A_k}}, \tag{38}$$

by substituting it for every k segments, for distance $\overline{D^J D^{J'}}$ the following can be obtained:

$$\delta_{xb}^{j} = \frac{1{,}2F_{NJ}^{j} \cdot cos\gamma_J^{j}}{G} \sum_{k=1}^{N} \frac{s_k}{\overline{A_k}}, \tag{39}$$

and for angular rotation:

$$\theta_{J1}^{j} = 0. \tag{40}$$

Displacement arising from shearing in the direction of the line of contact is:

$$\delta_{Jb}^{j} = \delta_{xb}^{j} \cdot cos\gamma_J^{j} = \frac{1{,}2F_{NJ}^{j} \cdot cos^2\gamma_J^{j}}{G} \sum_{k=1}^{N} \frac{s_k}{\overline{A_k}}. \tag{41}$$

### 4.4. Fillet-foundation deflection

The relative slender tooth connects to a bulky gear body. Connection of the gear body and the tooth has certain flexibility. If the tooth is considered to be rigid then displacement of work point $J^j$ also arises from fillet-foundation deflection as a consequence of angular rotation of the tooth. Deformation is generated by the effect of moment $F_{NJ}^{j}\left[cos\gamma_J^{j} \cdot \left(y_J^{j} - y_F\right) - sin\gamma_J^{j} \cdot x_J^{j}\right]$.

For displacement as a result of the moment we get [14]:

$$\delta_{xc}^{j} = \frac{1{,}327F_{NJ}^{j} \cdot \left[cos\gamma_J^{j} \cdot \left(y_J^{j} - y_F\right) - sin\gamma_J^{j} \cdot x_J^{j}\right] \cdot \left(y_J^{j} - y_F\right)}{E_v \cdot x_F^2 \cdot b}, \tag{42}$$

for angular rotation:

$$\theta_{J1}^{j} = \frac{1{,}327F_{NJ}^{j} \cdot \left[cos\gamma_J^{j} \cdot \left(y_J^{j} - y_F\right) - sin\gamma_J^{j} \cdot x_J^{j}\right]}{E_v \cdot x_F^2 \cdot b}. \tag{43}$$

Displacement in the direction of the line of contact:

$$\delta_{Jc}^{j} = \frac{1{,}327F_{NJ}^{j} \cdot \left[cos\gamma_J^{j} \cdot \left(y_J^{j} - y_F\right) - sin\gamma_J^{j} \cdot x_J^{j}\right]^2}{E_v \cdot x_F^2 \cdot b}. \tag{44}$$

### 4.5. Contact deflection

Conjunct deformation arising from flattening of the mating tooth pair can be determined according to [15] assuming that tooth are replace by cylinders with radii corresponding to them circles of curvature. Approach of the two cylinders is:

$$\delta_{Jd1,2}^{j} = \frac{3 \cdot 10^{-4} \cdot \varepsilon_{Ev}^{2,7} \cdot {F_{NJ}^{j}}^{0,9}}{{b_{1,2}}^{0,8}}, \tag{45}$$

where $b_{1,2}$ is the common tooth width of the contacting teeth,

$$\varepsilon_{Ev} = \sqrt[3]{\frac{11{,}5(E_{v1} + E_{v2})}{E_{v1} \cdot E_{v2}}}, \tag{46}$$

where

$$E_{v1,2} = \frac{2 \cdot E_{v1} \cdot E_{v2}}{E_{v1} + E_{v2}}. \tag{47}$$

So for eq. (45) we get:

$$\delta^{j}_{Jd1,2} = \frac{2{,}55 \cdot {F^{j}_{NJ}}^{0{,}9}}{E^{0{,}9}_{v1,2} \cdot b^{0{,}8}_{1,2}}, \tag{48}$$

where $F^{j}_{NJ} = 0{,}5F_{NJ}$ supposing contact of two teeth.

## 5. DETERMINATION OF THE MESHING STIFFNESS

According to the deflections specified in Section 4 meshing stiffness can be determined.

Meshing stiffness arising from bending deflection is given by:

$$k^{j}_{Ja} = \frac{F^{j}_{NJ}}{\delta^{j}_{Ja}}. \tag{49}$$

Meshing stiffness arising from shearing deflection is given by:

$$k^{j}_{Jb} = \frac{F^{j}_{NJ}}{\delta^{j}_{Jb}}. \tag{50}$$

Meshing stiffness arising from fillet-foundation deflection is given by:

$$k^{j}_{Jc} = \frac{F^{j}_{NJ}}{\delta^{j}_{Jc}}. \tag{51}$$

Meshing stiffness arising from contact deflection is given by:

$$k^{j}_{Jd1,2} = \frac{F^{j}_{NJ}}{\delta^{j}_{Jd1,2}}. \tag{52}$$

For one pair of teeth in contact the summarized meshing stiffness can be calculated from the sum of the individual meshing stiffness (15-18):

$$k^{j}_{1,2} = k^{j}_{J1,abc} + k^{j}_{J2,abc} + k^{j}_{J1,2}. \tag{53}$$

As deflections are continuously changing during the meshing cycle, so meshing stiffness changes too.

### 5.1. More than one tooth pair in contact

Of course there are cases when more than one tooth pair is in contact. The mating tooth pairs are individually modelled by springs connected in parallel (See *Figure 5*), so for the entire contact can be treated as a spring system [12]. In this case the components of the load should be divided between the tooth pairs. Determination of this division is subject to an individual study. After specifying this division the fore-presented method can be employed for the individual springs ($k_1$, $k_2$,…, $k_n$) and the resultant mesh stiffness can be calculated according to the following equation:

$$k_{\Sigma} = k_1 + k_2 + \cdots + k_n \,. \tag{54}$$

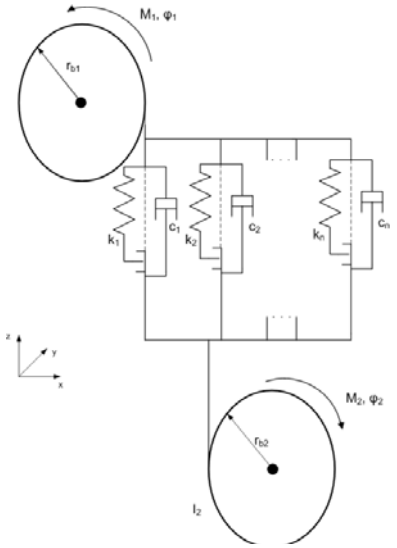



*Figure 5. Modified model*

## 6. CONCLUSION

For calculation of meshing stiffness of involute spur gears an analytical method is presented in this work. Based on the proposed method a computer program computing deflections is possible. The goal of this work is to integrate results of Section 4 into dynamic analysis and thus connect gear kinematics with gear dynamics. Of course verification of these results should be done by measurements and by FEM analysis. Aim of the authors to accomplish these confirmation steps in further studies.

Our calculation method for determining the contact points of gears with involute profile is a special one and have not adopted in studies [2-9].

Comparing our analytical methods with papers [2-9], calculation of the individual deflection components differs. Considering the method itself, the most similar method can be found in works [2-3], but there are differences in the obtained formulas of the individual deflection components. In works [2, 3] bending and shearing deflection is calculated jointly, and the applied model of the Hertzian contact also disagrees.

**Acknowledgement**

"This research was carried out as part of the TAMOP-4.2.1.B-10/2/KONV-2010-0001 project with support by the European Union, co-financed by the European Social Fund."

**References**

[1] F. L. Litvin: *A fogaskerék kapcsolódás elmélete.* Műszaki Könyvkiadó, Budapest, 1972.
[2] F. Chaari–W. Baccar–M. S. Abbes–M. Haddar: *Effect of spalling or tooth breakage on gear-mesh stiffness and dynamic response of a one-stage spur gear transmission.* European Journal of Mechanics A/Solids 27 (2008), pp. 691–705.
[3] F Chaari–T. Fakhfakh–M. Haddar: *Analytical modelling of spur gear tooth crack and influence on gearmesh stiffness*. European Journal of Mechanics A/Solids (2009), pp. 461–468.
[4] K. Markovic–M. Franulovic: *Contact stresses in gear teeth due to tip relief profile modification*. Eng. Rev. 31–1. 2011. pp. 19–26.
[5] J.J. Zhang–I.I. Esat–Y.H. Shi: *Load analysis with varying mesh stiffness.* Computers and structures 70 (1999), pp. 273–280.
[6] J. Hedlund–A. Lehtovaara: *Modeling of helical gear contact with tooth deflection.* Tribology Internation 40, 2007. pp. 613–619.
[7] J. I. Pedrero–M. Pleguetuelos–M. Artés–J. A. Antona: Load *distribution model along the line of contact for involute external gears*. Mechanism and Machine Theory 45, 2010. pp. 780–794.
[8] L. Walha–T. Fakhfakh–M. Haddar: *Nonlinear dynamics of a two-stage gear system with mesh stiffness fluctuation, bearing felxibility and backlash*. Mechanism and Machine Theory 44, 2009. pp. 1058–1069.
[9] A. Andersson–L. Vedmar: *A dynamic model to determine vibrations in involute helical gears*. Journal of Sound and Vibration 260, 2003. pp. 195–212.
[10] G. Litak–M. I. Friswell: *Vibration in gear systems*. Chaos, Solitons and Fractals (2003), p.p. 795-800.
[11] R. Szűcs–L. Kamondi: *Fogaskerekek dinamikai vizsgálatának egy lehetősége*. Kolozsvár: Erdélyi Magyar Műszaki Tudományos Társaság, Műszaki Szemle, 2010. pp. 416–419.
[12] R. Szűcs–L. Kamondi: *Bevezetés a geometria dinamikai vizsgálatokra gyakorolt hatásába*. GÉP LXI. (2010/9-10.), Gépipari Tudományos Egyesület Műszaki Folyóirata, pp. 102–104.
[13] R. Szűcs–L. Kamondi: *Bevezetés a fogaskerék kapcsolódás végeselem módszerrel történő vizsgálati lehetőségeibe*. GÉP LXII. (2011/11), Gépipari Tudományos Egyesület Műszaki Folyóirata, pp. 37–39.
[14] James M. Gere–Barry J. Goodno: *Mechnanics of Materials, Eighth Edition*. 2009 Cengage Learning
[15] M. J. Puttock–E. G. Thwaite: *Elastic Compression of Spheres and Cylinders at Point and Line Contact*. National Standards Laboratory Technical Paper, No. 25, Commonwealth Scientific and Industrial Research Organization, Australia, Melbourne 1969.